

Facile one-pot synthesis of porous N-doped graphene based NiO composite for parabens removal from wastewater and its reusability

Dalal Z. Husein*

Chemistry Department, Faculty of Science, New Valley University, El-Kharja, Egypt,
emails: dalal_husein@scinv.au.edu.eg, dalal_husein@yahoo.com

Received 10 November 2018; Accepted 26 April 2019

ABSTRACT

Personal care products (PCPs) have a prospective influence on human health, and their vast use may cause health effects such as breast cancer. In that perspective, current study is focused on designing a porous N-doped graphene-NiO nano-composite for adsorption of PCPs. Facile, easy and green one-pot synthesis via electrochemical/microwave-assisted method was applied. One family, parabens, of PCPs has been selected to be removed from water. Methyl, ethyl, propyl and butyl parabens were removed in single and competitive adsorption systems. The kinetics, thermodynamics, equilibrium, and adsorption behavior under varied pH and dosage were investigated. Recycling of exhausted adsorbent was also studied. The adsorption amount of methyl, ethyl, propyl and butyl parabens was 3.12, 5.28, 8.42 and 10.46 mg g⁻¹ adsorbent under the optimum conditions. It was found that the process obeyed pseudo-second-order kinetic model and both Langmuir and Temkin isotherm models satisfactorily. The process was thermodynamically spontaneous and endothermic. Results revealed that the prepared adsorbent is recyclable and its removal mechanism involves hydrophobic as well as π - π interactions.

Keywords: Personal care products; Parabens; Adsorption; Graphene nanocomposite

1. Introduction

Parabens or alkyl esters of *p*-hydroxybenzoic acid have been deemed the most numerous organic compounds present as a preservative in many food, medicine, hygiene and diverse personal care products (PCPs) [1]. This is because of their effectiveness and low manufacturing costs. Parabens such as methylparaben (MP), ethylparaben (EP), propylparaben (PP) and butylparaben (BP) can damage the intracellular protein and the enzyme activity of microbes [2]. MP, EP, PP and BP have a prospective influence similar to estrogen, and their prolonged use may cause breast cancer. Municipal effluents have been identified as a major source of emerging pharmaceuticals and PCPs. People in households are either dumping PCPs in normal metabolism routes or dispose of expired PCPs into the toilets. Sometimes,

hospital effluents can contribute to the load due to irregular operations. PCPs are not biodegradable in the wastewater plants, and the domestic sewage will be then disposed into the natural environment [3]. Thus it is necessary to remove these compounds from the environment. Studies reported that graphene was effective material in removing organic pollutants from aquatic systems because of its hydrophobic surface and large surface area [4,5]. Since the isolation of graphene in 2004, considerable attention has been paid to explore its applications in the environment [6]. This is because of its unique physical and chemical properties. Graphene has a high surface area, high chemical stability and rapid charge carrier mobility. So far, different techniques have been carried out to synthesize graphene sheets such as chemical vapor deposition [7], micromechanical exfoliation

* Corresponding author.

of graphite [8], solvothermal synthesis [9], unzipping of carbon nanotubes [10] and microwave synthesis [11]. Among the various methods of graphene synthesis, electrochemical method is one of the simple, fast and high-yielding methods [12]. Graphene has a honeycomb lattice structure with single carbon nanosheets of two-dimensional (2D) sp^2 -hybridization. Many researchers have demonstrated that the chemical doping of graphene with foreign atoms can improve its properties [13]. Mono-heteroatom doped graphene, especially nitrogen-doped graphene has been identified as a good choice for adsorption, catalytic activity, desalination membranes and durability performance, the superiority result from enriched high nitrogen doping content and enlarged surface area [14–17]. Nitrogen for graphene is deemed a stellar dopant due to its comparable atomic size. In addition, strong bonds can be formed between the nitrogen lone pair electrons and the graphene π -electron system. This process leads to a significant increase in the spin density, electron conductivity and charge distribution of the carbon atoms, which led to the formation of an activation region on the surface of graphene. This, in turn, increases its ability to bind any guest molecules such as inorganic compounds [18]. Compared with active inorganic compounds metal oxides nanocomposites not only has excellent electrocatalytic activity and biocompatibility but also has the advantage of large surface area, which is useful for the adsorption process. The metal oxide nanoparticles act as a stabilizing agent against the aggregation of individual graphene layers, which occurred because of strong van der Waals forces between graphene sheets [19]. Studies conducted that the removal of the honeycomb lattices of graphene and form nanopores with specific size and geometry leads to increase the permeation ability of graphene [20]. It is reported that lightweight porous carbon materials, including graphene, exhibit distinct advantages regarding excellent electrical conductivity and chemical stability, over porous metals [21]. The *N*-doped graphene with a large pore volume and a high surface area result in high removal efficiency of contaminants and good recycling performance [22–24].

The chemical methods that used to produce graphene such as Hummer's method involve the production of graphene oxide. Hummer's method has many disadvantages such (a) using highly toxic and corrosive chemicals that induces severe environmental concerns, (b) the product is graphene oxide. To produce graphene, the graphene oxide produced must be reduced using reducing agents, and (c) the method is time-consuming. Hence, all these limitations lead to limit the large-scale production of graphene.

In this study, green, simple, efficient and affordable method for the synthesis of porous N grafted graphene-NiO nanoparticles is carried out. The as-prepared adsorbent is applied for removal of MP, EP, PP and BP from aqueous solution. In one-pot step graphite is exfoliated electrochemically into graphene sheets and modified to enhance its removal capacity via (i) doping with N, (ii) increasing its surface area by creating nanopores structure, and (ii) distributing NiO nanoparticles along graphene sheets surface. Parabens adsorption by porous N grafted graphene-NiO nanoparticles was investigated under various reaction conditions. Kinetic and thermodynamic studies were performed. Reusability

of the prepared adsorbent was also explored. The proposed adsorption mechanism has been discussed.

2. Experimental

2.1. Materials and instruments

Sodium salts of ethylparaben (EP), propylparaben (PP), methylparaben (MP) and butylparaben (BP) were provided by Bristol-Myers Squibb, Egypt. Nickel nitrate, glycine, sodium hydroxide and hydrochloric acid were of analytical reagent grade and used directly. The Brunauer–Emmett–Teller (BET) surface area measurements of the prepared composite were measured using ASAP 2000C, Micromeritics, USA. Transmission electron microscopy (TEM, JEOL; JEM-100 CXII, USA), Scanning electron microscopy (SEM, JEOL; JSM 5400LV, USA) and X-ray diffraction (XRD, Phillips; PW 1710, USA) analysis was also performed to study the properties and composition phases of the adsorbent. The spectrophotometer (PerkinElmer; LAMBDA 750, USA) was used to determine the concentrations of parabens contaminants.

2.2. Synthesis of porous *N*-doped graphene based NiO composite (NiO@N-G)

Electrochemical/microwave-assisted route is applied to produce nitrogen doped-graphene/NiO via exfoliation of graphite source in presence of nickel ions and glycine. The amino acid, glycine, was added to the solution phase to functionalize the resulted graphene with nitrogen. For electrochemical exfoliation of graphite and grafting of produced sheets at once, two pencil graphite rods (2 mm diameter) were dipped in 40 mL solution of 1.5 g $Ni(NO_3)_2 \cdot 6H_2O$ and 2 g of glycine under DC voltage (12 V). Both two pencil graphite rods were placed parallel at a distance of 2 cm from each other as shown in Fig. 1a. During the electrochemical exfoliation process, the anodic electrode was swelled and corroded as black precipitate and gradually appeared at the bottom in the electrolytic cell as dispersion that can be observed in Fig. 1b. After 3 h electrolysis, the exfoliated graphene reaction mixture was stirred and heated at 70°C till evaporation. Then the dried mass was subjected to a microwave oven for 3 min. The resulted solid foam (Fig. 1c) was crushed and subjected again to microwave radiation for 1 min.

2.3. Batch adsorption experiments

The uptake of parabens (EP, MP, BP and PP) from aqueous medium was studied in batch mode. All adsorption isotherm tests were carried out at room temperature, 23°C. The initial pollutant concentration and NiO@N-G dose were maintained constant at 10 mg L⁻¹ and 50 mg/20 mL, respectively. The effects of kinetic experiments at various contact time (0–90 min), adsorption isotherm at a various initial concentration (3–20 mg L⁻¹) and thermodynamic studies at various temperatures (296–311 K) on adsorption process were studied at optimum pH. Solutions of 0.1 M HCl and NaOH were used for adjusting the pH value of sample. The competitive adsorption experiment was carried out using mixed parabens concentration of 10 mg L⁻¹ and 50 mg/20 mL adsorbent dose at room temperature. After adsorption/

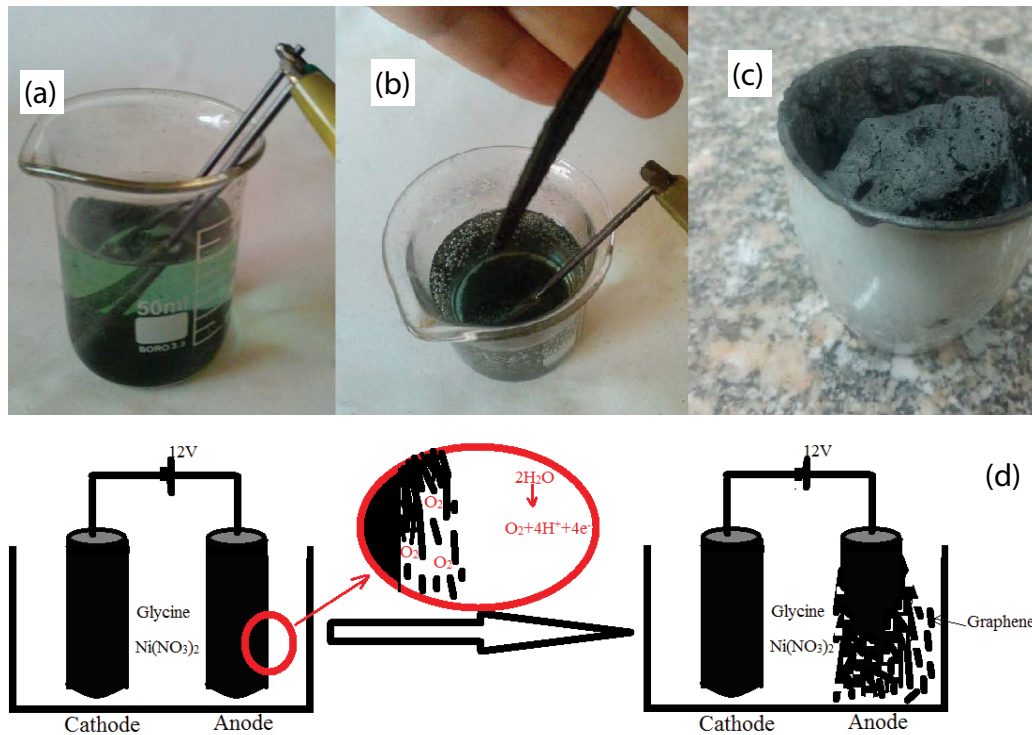


Fig. 1. Exfoliation of graphite into graphene under 12 V DC and using nickel nitrate as electrolyte in presence of glycine (a and b), the resulted NiO@N-G foam (c) and electrochemical exfoliation of anodic graphite into graphene (d).

desorption equilibrium is reached (3 h), the concentrations of EP, MP, BP and PP were determined and the adsorption capacity, q_e (mg g^{-1}) of NiO@N-G adsorbent was calculated as:

$$q_e = (C_0 - C_e) \times \frac{V}{m} \quad (1)$$

where C_e and C_0 are the equilibrium and initial parabens concentration. The repeated use and desorption experiments were performed using ethanol in the concentration range of 0%–100%. A 250 mg of NiO@N-G adsorbed with contaminant was shaken with ethanol (100 mL) at 150 rpm, and allowed for a time period up to 6 h at room temperature. The percentage of parabens desorbed from NiO@N-G is calculated as:

$$\text{Desorption (\%)} = \left(\frac{\text{Mass of paraben desorbed}}{\text{Mass of paraben absorbed}} \right) \times 100\% \quad (2)$$

2.4. Isotherm model

It shows the relationship between the pollutant (parabens) concentration in the solution and that on NiO@N-G surface at given equilibrium conditions. Freundlich, Langmuir, Temkin and Dubinin–Radushkevich (D-R) isotherms were used to represent the obtained sorption data. The following expression is used to calculate the Langmuir isotherm [25]:

$$\frac{C_e}{q_e} = \left(\frac{1}{q_L K_L} \right) + \left(\frac{1}{q_L} \right) \times C_e \quad (3)$$

where q_L is the sorption capacity of NiO@N-G, mg g^{-1} , and K_L is the Langmuir constant, L mg^{-1} .

Freundlich model was calculated as [26]:

$$\log q_e = \log K_F + \left(\frac{1}{n} \right) \log C_e \quad (4)$$

where K_F and $1/n$ are Freundlich constants related to adsorption capacity and the heterogeneity factor, respectively.

Temkin model was calculated as [27]:

$$q_e = B \ln A + B \ln C_e \quad (5)$$

where

$$B = \frac{RT}{b} \quad (6)$$

where A , $\text{L mg}^{-1} \text{m}^{-1}$, and B are Temkin constants related to the equilibrium binding and the adsorption heat. R is the gas constant where T is the absolute temperature.

The D-R model was calculated from the following relation [28]:

$$\ln q_e = \ln q_m - \beta \varepsilon^2 \quad (7)$$

where β is a D-R coefficient related to the free energy, E (kJ mol^{-2}), of adsorption process and equal to $(0.5 \beta)^{0.5} = (\sqrt{1/2\beta})$, q_m is the D-R maximum adsorption capacity and ε , J mmol^{-1} , is the Polanyi potential that can be given as:

$$\varepsilon = RT \left(\frac{1+1}{C_e} \right) \quad (8)$$

2.5. Kinetic studies

To study the kinetics of NiO@N-G nanocomposite, pseudo-first, pseudo-second-order, Elovich and intraparticle diffusion kinetic model were tested.

Pseudo-first-order model [29]:

$$\log(q_e - q_t) = \log q_e - \left(\frac{K_1}{2.303}\right) \times t \quad (9)$$

where K_1 (min^{-1}) denoted the constant of pseudo-first-order rate.

Pseudo-second-order [30]:

$$\frac{t}{q_t} = \frac{1}{(K_2 q_e^2)} + \left(\frac{1}{q_e}\right) \times t \quad (10)$$

where K_2 , $\text{g mg}^{-1} \text{min}^{-1}$, denoted the constant of pseudo-second-order rate of parabens adsorption onto NiO@N-G.

Elovich model [31]:

$$q_t = \frac{1}{\beta} \ln(\alpha\beta) + \left(\frac{1}{\beta}\right) \ln t \quad (11)$$

where β , g mg^{-1} , is a constant related to the magnitude of NiO@N-G surface coverage and activation energy for chemisorptions and α , $\text{mg g}^{-1} \text{min}^{-1}$, donated the initial rate constant.

The intraparticle diffusion model [32]:

$$q_e = C + k_{\text{int}} t^{\frac{1}{2}} \quad (12)$$

where K_{int} and C are constants calculated from the plot of q_e vs. $t^{1/2}$.

2.6. Thermodynamic study

Thermodynamic behavior of parabens/NiO@N-G adsorption system was calculated as:

$$\Delta G^\circ = -RT \ln K_C \quad (13)$$

$$\ln K_C = -\frac{\Delta G^\circ}{RT} = -\left(\frac{\Delta H^\circ}{RT}\right) + \left(\frac{\Delta S^\circ}{R}\right) \quad (14)$$

$$K_C = \frac{C_e}{C_o} \quad (15)$$

where ΔG° , kJ mol^{-1} , is the Gibbs free energy, ΔH° , kJ mol^{-1} , is the enthalpy, ΔS° , $\text{J mol}^{-1} \text{K}^{-1}$, is the entropy, K_C is the thermodynamic equilibrium constant and C_o is mg of parabens adsorbed per liter.

3. Results and discussion

3.1. Electrochemical exfoliation of graphite into graphene

When the voltage (12 V) is applied to the graphite electrodes, the surface of the electrode becomes wet with the electrolyte and anodic graphite electrode expands due to

intercalation. Subsequently, the graphite flakes are continuously expanded and peeled. Water in the electrochemical process is very important as the formation of “broken” graphene layers basically originate from the interaction of water molecules on widened graphite, which was electrochemically exfoliated by the generation and evolution of gases such as O_2 . The electrolysis of H_2O induces the corrosion of edges sites and grain boundaries which result in expanding the graphite, facilitating the intercalation and peeling of graphene layers [33]. Graphene produced using electrochemical exfoliation technique can be of relatively high quality and the level of defects in such graphene is lower than in reduced graphene oxide that produced by conventional chemical methods such as Hammer’s method [34]. Fig. 1d demonstrates the anodic exfoliation of graphite electrode into graphene.

3.2. Characterization of NiO@N-G

The XRD pattern of the as-obtained NiO@N-G is explained in Fig. 2a. The diffraction peaks at $2\theta = 37.8^\circ$, 44.1° , 64.2° and 77.2° are assigned to (111), (200), (220) and (311), respectively. Such crystalline structure of nickel oxide suggested that the resulting NiO in NiO@N-G composite is face-centered cubic (JCPDS 47–1049). The peak at $2\theta = 26.4^\circ$ is the typical diffraction peak (002) of the graphitic character of graphene sheets, indicated that the NiO nanocrystallites have not greatly influenced the orientation of the graphene layers.

Thermogravimetric analyzer (TGA) measurements were carried out in order to determine the weight percentage of NiO in the NiO@N-G, and the thermal stability of the nanocomposites. As depicted in Fig. 2b, the slight weight loss (about 10 wt.%) below 200°C for as-obtained NiO@N-G is mainly ascribed to the volatilization of absorbed water. About 33 wt.% residue is obtained after the thermal decomposition. Meanwhile, the TGA curve indicates a mean weight loss of 57 wt.% at about 450°C , which can be related to combustion of the N-G. The amount of nitrogen and its presence in nanocomposite was confirmed using CHNS analysis and FT-IR spectroscopy, respectively. The CHNS analysis of NiO@N-G revealed that the N wt.% is 12%. The presence of nitrogen in NiO@N-G is supported by FTIR-band (C–N) at $1,438 \text{ cm}^{-1}$ (Fig. 2c). The absorption band at $1,620 \text{ cm}^{-1}$ is attributed to the presence of C=C stretching of the aromatic ring. In addition, the broad absorption band around $3,412 \text{ cm}^{-1}$ is assigned to O–H and N–H stretching vibration.

The SEM image, Fig. 2d, demonstrated an irregular surface with high porosity and roughness. The specific surface area for the NiO@N-G was found to be $227.5 \text{ m}^2 \text{g}^{-1}$ as obtained by the BET calculations. As shown in Fig. 2e, the black NiO nano-particles are anchored on the gray thin graphene sheets. Based on the TEM analysis, the particle size of NiO in the as-obtained composite is between 11 and 24 nm, in accord with the XRD analysis result using the Scherrer’s equation.

3.3. Effect of absorption conditions

3.3.1. Effect of solution pH on parabens adsorption onto NiO@N-G

Fig. 3a depicts the pH effect on parabens adsorption by NiO@N-G. Generally, solution pH affects the surface charge

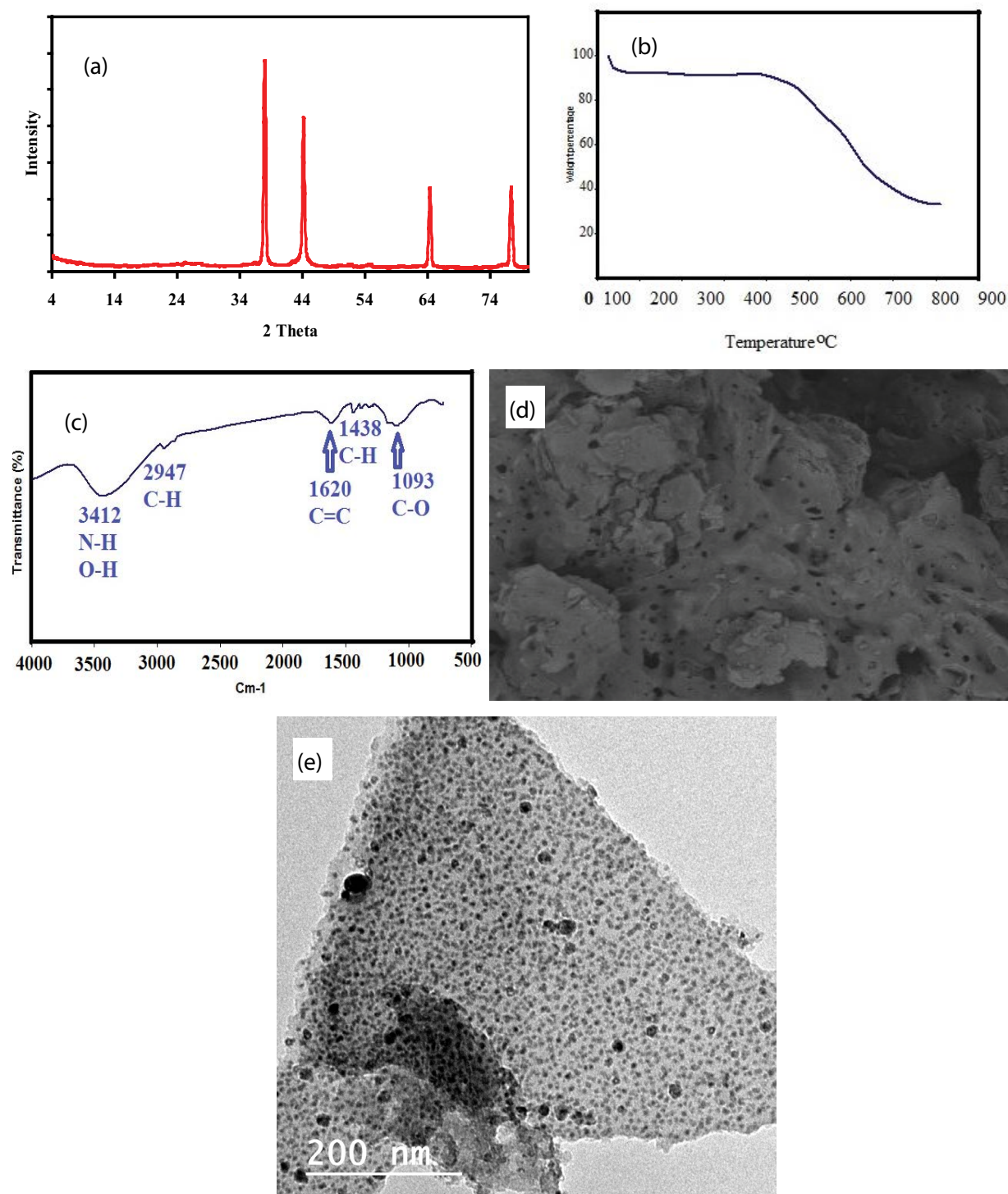


Fig. 2. Characterization of NiO@N-C composite; XRD analysis (a), TG curve (b), FTIR analysis (c), SEM (d) and TEM analysis (e).

of the adsorbent material and the degree of ionization of the pollutant [35]. As presented in Fig. 3a, the parabens removal was the maximum when the pH was 5. A similar trend of pH effect was observed for the removal of methyl parabens onto polyacrylonitrile beads [36]. After pH 5, the adsorption efficiency decreased. The removal efficiency of parabens (as phenolic contaminants) was determined by their

pKa vs. the pH of the solution [37]. Therefore, at $\text{pH} > 5$ ($\text{pH} > \text{pKa}$) the surface of graphene was negatively charged so the electrostatic repulsion between the negatively charged graphene and the dissociated parabens increased. The dissociation of the $-\text{OH}$ group of parabens increased their hydrophilicity and form hydrogen bonding between graphene and parabens, thereby the uptake decreased at

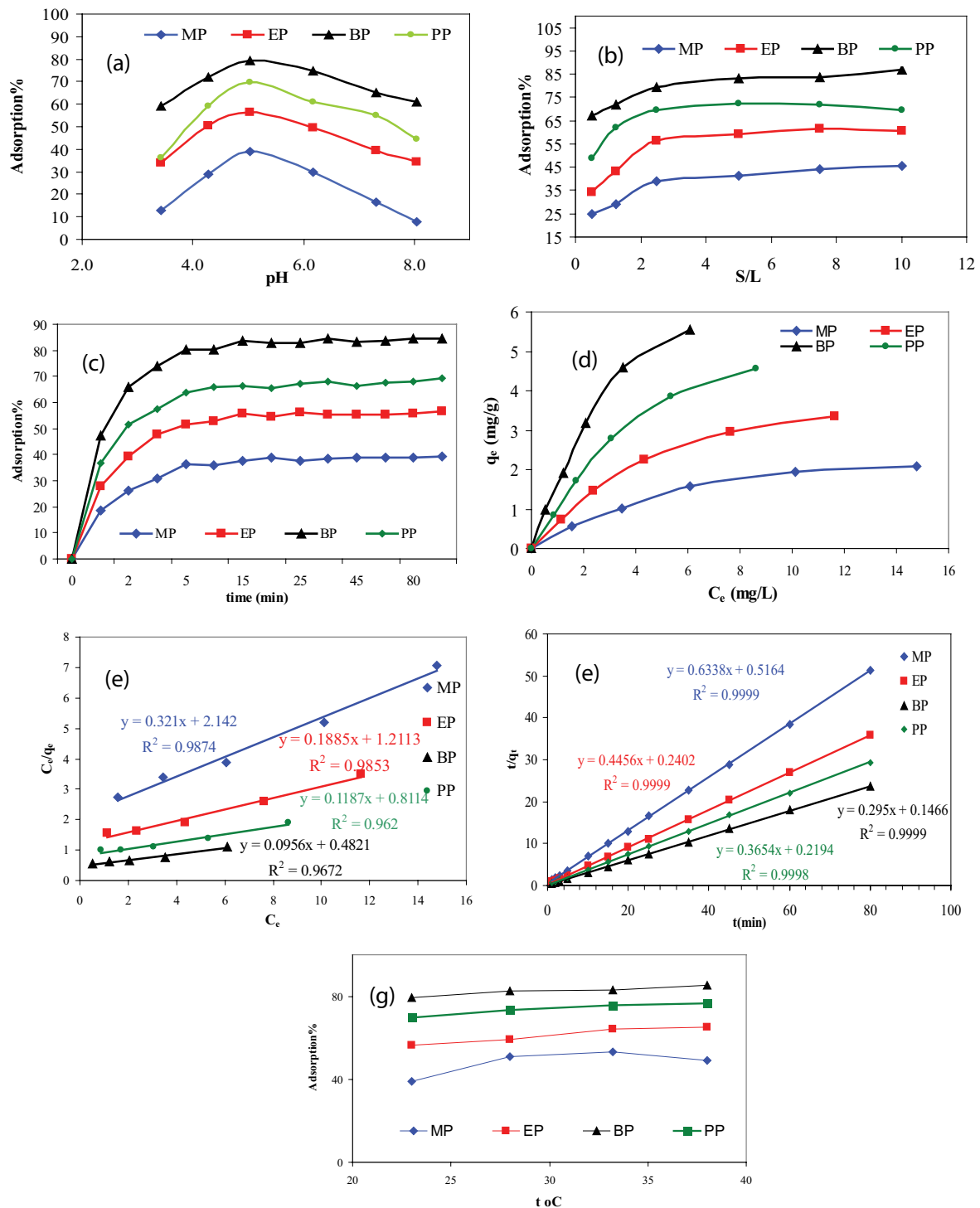


Fig. 3. Adsorption of parabens onto NiO@N-G; effect of pH (a), solid/liquid ratio (b), contact time (c), adsorption isotherm (d), Langmuir model (e), pseudo-second-order kinetic model (f) and temperature effect (g).

$pH > pK_a$ [38]. The adsorption of parabens into graphene with increasing pH before their pK_a may be related to the enhanced π - π electron donor-acceptor interactions [37]. The results showed that the removal% of NiO@N-G followed the order of MP (39.20%) < EP (56.57%) < PP (69.50%) < BP (79.30%). Such finding may be attributed to

the hydrophilic and hydrophobic properties. According to the solubility, the hydrophobicity followed the same order (MP < EP < PP < BP). The molecular weight also followed the same previous order arrangement which assures that adsorption affinity of parabens increased as the bulkiness of molecule increased.

Taking into account that optimum pH is 5, henceforth all experiments have been carried out at pH 5.0.

3.3.2. Effect of solid/liquid ratio on adsorption of parabens onto NiO@N-G

The removal of parabens by NiO@N-G was presented in Fig. 3b. With the increase in NiO@N-G dosage, the adsorption of parabens increased. Keeping parabens concentrations fixed at 10 mg L⁻¹ and increasing the NiO@N-G solid/liquid (S/L) ratio, makes a large number of active sites available for a fixed parabens concentration, hence the increase in the extent of uptake. The uptake increased rapidly till the S/L ratio of 2.5, after that the increase in adsorption was insignificant. Thus the S/L 2.5 was chosen to perform the rest of the experiments.

3.3.3. Effect of contact time

Fig. 3c represents the effect of contact time on the parabens adsorption at various contact time. In the initial stages, the saturation curves rise sharply suggesting that plenty of active sites are available. As illustrated in Fig. 3c about 15 min is needed for parabens to achieve adsorption equilibrium. A plateau is achieved in all parabens curves suggesting that the NiO@N-G is saturated at this level, eventually. The uptake curves are smooth, single and continuous, indicating monolayer coverage of parabens onto the NiO@N-G composite surface. The % removal follows the order MP < EP < PP < BP, that is, the same order of increasing of molecular weight.

3.4. Adsorption isotherms

Experimental data gained from the parabens/NiO@N-G experiments were subjected to four isotherm models, Freundlich, Temkin, Langmuir and D-R. From Fig. 3d and Table 1, Langmuir isotherm model fit well the obtained data with high R^2 , regression coefficient, the value of 0.99, 0.99, 0.96 and 0.97 for MP, EP, PP and BP, respectively. The best fit to Langmuir model depicted that parabens sorption was a monolayer and NiO@N-G provided the specific homogeneous sites (Fig. 3e). The calculated maximum adsorption capacity (q_m) of parabens/NiO@N-G at room temperature followed the order: MP (3.12 mg g⁻¹) < EP (5.28 mg g⁻¹) < PP (8.42 mg g⁻¹) < BP (10.46 mg g⁻¹) in accordance with previous results on the effect of pH. In fact, there are limited publications for parabens removal from water. However, the obtained maximum capacities in this study were compared with the available studies. It was found that the maximum adsorption capacities obtained in this study were consistent with those obtained by Forte et al. [36] and Chen et al. [39].

The Langmuir equilibrium parameter, R_L , was calculated by the following relation and represented in Table 1:

$$R_L = \frac{1}{(1 + K_L C_{\max})} \quad (16)$$

where C_{\max} is the highest concentration of parabens. The values of R_L were found to be less than 1 for all parabens removal by NiO@N-G; which indicate that the adsorption process is favorable.

Table 1
Calculated parameters for each isotherm used in this study

Isotherm model	Pollutant	Parameter	R^2	
Langmuir	MP	q_L	3.12	0.99
		K_L	0.15	
	EP	q_L	5.28	0.99
		K_L	0.16	
	PP	q_L	8.42	0.96
		K_L	0.15	
	BP	q_L	10.46	0.97
		K_L	0.20	
Freundlich	MP	K_F	0.47	0.97
		n	1.68	
	EP	K_F	1.31	0.96
		n	1.51	
	PP	K_F	1.08	0.97
		n	1.37	
	BP	K_F	1.66	0.98
		n	1.35	
Temkin	MP	A	1.36	0.99
		B	0.71	
	EP	A	1.60	0.99
		B	1.16	
	PP	A	1.81	0.97
		B	1.66	
	BP	A	1.83	0.96
		B	1.98	
D-R	MP	q_m	1.837	0.905
		E	0.001	
	EP	q_m	2.90	0.93
		E	0.0005	
	PP	q_m	3.88	0.93
		E	0.0005	
	BP	q_m	4.55	0.90
		E	0.0004	

However, the Temkin isotherm model is suitable for adsorption based on strong electrostatic interactions [40]. To confirm the existence of electrostatic interactions, The Temkin isotherm model was explored to analyze the adsorption data and it was found that R^2 values were 0.99, 0.99, 0.97 and 0.96 for MP, EP, PP and BP, respectively. Therefore, Temkin model also provided a suitable fit indicated that electrostatic interactions exist between parabens and nanocomposite. The values of constants of Langmuir, Freundlich, Temkin and D-R models are presented in a tabulated form in Table 1. In the energy parameter isotherm models, Temkin and D-R were used to present heat of sorption (B), mean free energy (E) and sorption energy value (β). As listed in Table 1, $B < 20$ kJ mol⁻¹ and $E < 8$ which is an indication that physisorption dominates chemisorption and ion exchange.

3.5. Adsorption kinetics

Adsorption kinetics is important to describe the adsorption process proceedings. The uptake of parabens by the NiO@N-G adsorbent displayed that sorption equilibrium had been reached after 15 min. Four kinetic models, pseudo-first, second-order, Elovich and intraparticle diffusion, were used to analyze experimental data at room temperature. As shown in Fig. 3f and Table 2, the pseudo-second-order kinetic model best fitted the parabens/NiO@N-G system with R^2 , correlation coefficient, value 1 and q_e (mg g^{-1}) were 1.58, 2.24, 2.74 and 3.39 for MP, EP, PP and BP, respectively. These calculated values of q_e were close to the experimental ones, that is, 1.57, 2.26, 2.78 and 3.38 for the same order.

For the Elovich model, β value is an indication of the active sites available for parabens adsorption while α is the uptake quantity of parabens at 1 min (when $\ln t = 0$). Such α value is beneficial in recognizing the sorption manner of the first step. As shown in Table 2, it is clear that the Elovich model suits the obtained data worse than the pseudo-second-order kinetic model.

Typical sorption system includes three basic steps: liquid film diffusion, intraparticle diffusion and mass action. For physical sorption process, the mass transfer is fast and very small in the kinetic studies. Consequently, film diffusion or intraparticle diffusion step is controlling the adsorption kinetics. Hence the intraparticle diffusion model was explored. In the intraparticle diffusion model, there are two linear behaviors suggesting that the adsorption process consists of surface sorption and intraparticle diffusion. The first linear part of the plot is related to boundary layer effect (surface sorption) while the second linear part is indicative for intraparticle diffusion. The values of K_{int} , intraparticle diffusion rate together with the C and R^2 values, are presented in Table 2. The C value provides information about the thickness of the surface adsorption layer (boundary layer). As reported in Table 2, a non-zero value of C constant proposed that parabens removal by NiO@N-G was not only depended on intraparticle diffusion but also involves numerous complex adsorption mechanism of mass action [41].

3.6. Thermodynamic studies

Enthalpy (ΔH°), Gibbs free energy (ΔG°) and entropy (ΔS°) were calculated and recorded in Table 3. The negative values of ΔG° indicated the spontaneity of parabens adsorption onto NiO@N-G surface (Fig. 3g). The positive values of enthalpy, ΔH° , confirmed the endothermic process while positive values of entropy, ΔS° , denoted randomness at the NiO@N-G/parabens interface. Each parabens molecule exists in aqueous solution had to exchange more than one water molecule before being adsorbed by NiO@N-G material. Furthermore, the calculated values of ΔH° listed in Table 3 ($<20.9 \text{ kJ mol}^{-1}$), confirmed the physical adsorption process [41].

3.7. Competitive adsorption behavior

The single-solute adsorption behavior is not meaningful for predicting contaminant removal in real environments since co-occurrence is common. It was found that the

Table 2

Obtained kinetic parameters for each model used

Kinetic model	Pollutant	Parameter		R^2
Pseudo-first-order	MP	q_e	0.95	0.72
		K_1	1.45	
	EP	q_e	0.14	0.43
		K_1	0.04	
	PP	q_e	9.59	0.58
		K_1	0.06	
	BP	q_e	0.83	0.63
		K_1	0.06	
Pseudo-second-order	MP	q_e	1.58	1.00
		K_2	0.78	
	EP	q_e	2.24	1.00
		K_2	0.83	
	PP	q_e	2.74	1.00
		K_2	0.59	
	BP	q_e	3.39	1.00
		K_2	0.59	
Elovich	MP	α	77.06	0.78
		β	6.26	
	EP	α	247.28	0.74
		β	4.74	
	PP	α	948.54	0.74
		β	4.38	
	BP	α	3,182.12	0.70
		β	3.84	
Intraparticle diffusion	MP	K_{int}	0.07	0.54
		C	1.08	
	EP	K_{int}	0.09	0.49
		C	1.62	
	PP	K_{int}	0.03	0.49
		C	0.60	
	BP	K_{int}	0.12	0.46
		C	2.61	

adsorption removals of each paraben in a single sorption solution are higher compared with the removal efficiency of each paraben in mix solution. However, the total adsorption capacity of the four parabens was higher than that of each paraben single system, suggesting that the removal capacity of NiO@N-G was increased for the coexisting multi-paraben components. The adsorption efficiency of BP, PP, EP and MP reduced by 1.2%, 5.1%, 9.4% and 15.3%, respectively, in the mix solution. This is due to competitive adsorption between various paraben molecules adsorbed on the surface of the NiO@N-G composite. Moreover, the results indicate that the coexistence of the four paraben molecules suppresses MP and EP sorption more significantly but has little effect on PP and BP adsorption. It was found that the adsorption uptake increases with decreasing of parabens polarity in the

Table 3
Thermodynamic parameters of parabens adsorption onto NiO@N-G

Pollutant	T (K)	K_c	ΔG° (kJ mol ⁻¹)	ΔH° (kJ mol ⁻¹)	ΔS° (J mol ⁻¹ K ⁻¹)	R^2
MP	296	0.64	1.08	20.70	69.17	0.48
	301	1.04	-0.11			
	306	1.15	-0.35			
	311	0.97	0.07			
EP	296	1.30	-0.65	19.87	69.32	0.97
	301	1.46	-0.95			
	306	1.78	-1.46			
	311	1.88	-1.63			
BP	296	3.83	-3.31	19.83	78.36	0.94
	301	4.75	-3.90			
	306	4.92	-4.06			
	311	5.85	-4.57			
PP	296	2.28	-2.03	18.77	70.56	0.94
	301	2.77	-2.55			
	306	3.13	-2.91			
	311	3.29	-3.08			

order BP (78.1%) > PP (64.4%) > EP (47.2%) > MP (23.9%). Butylparaben shows the highest removal either in a single solution or a mixture of parabens. This may be due to the higher hydrophobicity of BP compared with other paraben molecules as the BP is the least polar and least soluble in water. Hence, BP can easily attract into the active sites of nano-composite due to the strongest parabens–NiO@N-G interaction. The increased amounts of BP, PP, EP and MP on NiO@N-G at multi-system could be assigned to the intramolecular interactions between parabens themselves.

3.8. Possible adsorption mechanism

The adsorption mechanism between graphene and organic pollutant depends mainly on the structure of contaminant and active sites of the graphene. Yu et al. [37] proposed and elucidated the adsorption mechanism between phenolic contaminants and graphene based materials, in which the π - π interactions, hydrogen bonding and hydrophobicity were considered to be important parameters in the adsorption process. The removal efficiency of NiO@N-G composite toward butylparaben removal seemed to be better than of propylparaben, followed by ethylparaben, followed by that of methylparaben. Due to the hydrogen bonding between O-containing groups of graphene and hydroxyl groups in BP, PP, EP and MP, the -OH groups of different paraben molecules were preferentially attracted to graphene surfaces and left the hydrophobic part (alkyl benzene) to face the solution. The hydrophobic part of parabens could supply new active sites; whereby a second layer of parabens would be adsorbed to the previously adsorbed paraben molecules by hydrophobic as well as π - π interactions [42]. The hydrophobicity relays on the alkyl chain in the parabens, whereas longer alkyl chain leads to higher hydrophobicity and therefore higher affinity to attract to the nanocomposite

surface. The polarizability of parabens increases in the order: BP > PP > EP > MP due to increase of molecular weight in the same order. BP has the largest molecular weight thus has the greatest dispersive force with highly polarizable graphene sheets. Therefore, the adsorption efficiency of four parabens compounds on graphene was in the order BP > PP > EP > MP. The hydrophobicity relays on the alkyl chain in the parabens, whereas longer alkyl chain leads to higher hydrophobicity and therefore higher affinity to attract to the nanocomposite surface. Besides, π - π interactions that occur via double bonds of graphene sheets and those (benzene rings) in the parabens.

3.9. Repeated use and desorption studies

The regeneration ability of given adsorbent is vital and important for practical applications as it controls the overall cost for the adsorbent. The adsorbed parabens, MP, EP, PP and BP onto NiO@N-G were desorbed by using different ethanol concentrations (0%–100%) at room temperature and time of 6 h. As demonstrated in Figs. 4a and b, the released amounts of parabens increased with the increase in ethanol concentration greatly. The desorption efficiency (%) was 50.1% MP, 81.1% EP, 99% PP and 99.9% BP when the ethanol concentration was 100%. Such finding synchronized with hydrophobicity phenomenon which follows the same order. The results also revealed that the adsorption of PP and BP into NiO@N-G material was totally reversible. This means the bonding between NiO@N-G and both PP and BP are weak. To evaluate the performance of NiO@N-G as an adsorbent, one key factor is important, reusability. The adsorption–desorption cycle was repeated four times and the reusability reached 91.5%. Thus it can conclude that the NiO@N-G adsorbent is recyclable and is stable during the process.

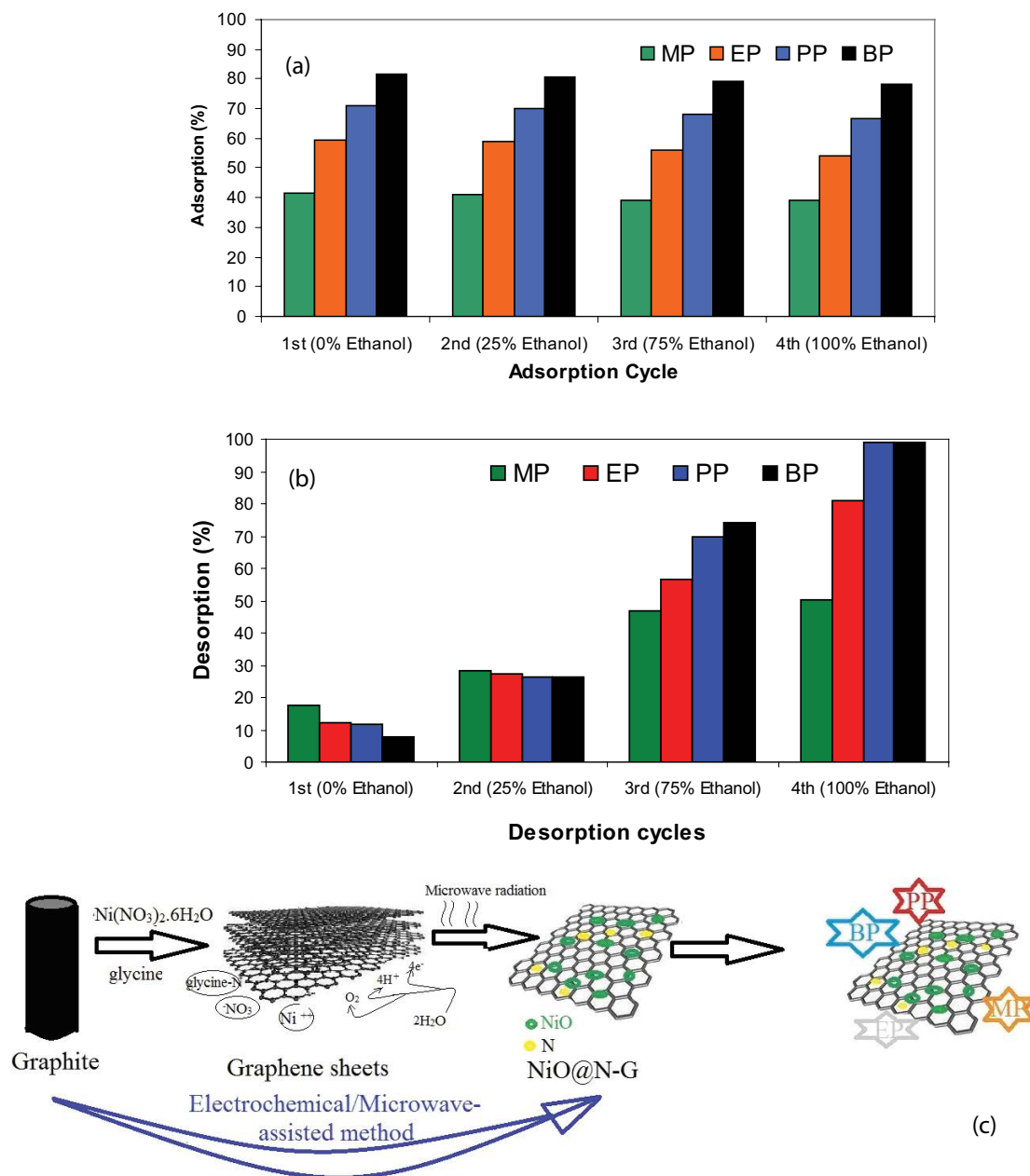


Fig. 4. Adsorption (a) and desorption (b) consecutive cycles for parabens; MP, EP, PP and BP onto NiO@N-G at different water: ethanol ratio; Graphical abstract for NiO@N-G preparation and removal of parabens (c).

4. Conclusion

This study presents a cost effective, cheap and easy method to synthesize NiO@N-G by electrochemical exfoliation in presence of nickel salt as electrolyte and glycine as a source of nitrogen. The electrochemical route is quite simple, green and fast to synthesize graphene sheets directly with high quality in mass production. The study shows that NiO@N-G can be used to remove MP, EP, PP and BP from aqueous solutions efficiently. Graphical abstract for NiO@N-G preparation and removal of parabens is presented in Fig. 4c. The adsorption characteristics of parabens/NiO@N-G system in water are influenced by several factors.

The adsorption was highly dependent on pH, reaction temperature and NiO@N-G dosage. Results showed that the adsorbed amount of parabens was the maximum at pH 5 and the process was thermodynamically spontaneous and endothermic. Kinetic studies denoted that the process followed the pseudo-second-order model. Both Temkin and Langmuir isotherms described well the sorption process. The present study concluded that the NiO@N-G adsorbent was a very suitable material for the simultaneous removal of organic pollutants. In addition, NiO@N-G is stable and recyclable without significantly losing its adsorption efficiency.

References

- [1] A.V.F. Sako, M.D. Dolzan, G.A. Micke, Fast and sensitive method to determine parabens by capillary electrophoresis using automatic reverse electrode polarity stacking mode: application to hair samples, *Anal. Bioanal. Chem.*, 407 (2015) 7333–7339.
- [2] Y. Okamoto, T. Hayashi, S. Matsunami, K. Ueda, N. Kojima, Combined activation of methyl paraben by light irradiation and esterase metabolism toward oxidative DNA damage, *Chem. Res. Toxicol.*, 21 (2008) 1594–1599.
- [3] T. Heberer, Occurrence, fate, and removal of pharmaceutical residues in the aquatic environment: a review of recent research data, *Toxicol. Lett.*, 131 (2002) 5–17.
- [4] Z. Pei, L. Li, L. Sun, S. Zhang, X.-q. Shan, S. Yang, B. Wen, Adsorption characteristics of 1,2,4-trichlorobenzene, 2,4,6-trichlorophenol, 2-naphthol and naphthalene on graphene and graphene oxide, *Carbon*, 51 (2013) 156–163.
- [5] J. Zhao, Z. Wang, Q. Zhao, B. Xing, Adsorption of phenanthrene on multilayer graphene as affected by surfactant and exfoliation, *Environ. Sci. Technol.*, 48 (2014) 319–331.
- [6] W. Yuan, J. Chen, G. Shi, Nanoporous graphene materials, *Mater. Today*, 17 (2014) 77–85.
- [7] K.S. Kim, Y. Zhao, H. Jang, S.Y. Lee, J.M. Kim, K.S. Kim, J.-H. Ahn, P. Kim, J.-Y. Choi, B.H. Hong, Large-scale pattern growth of graphene films for stretchable transparent electrodes, *Nature*, 457 (2009) 706–710.
- [8] Y. Zhu, S. Murali, W. Cai, X. Li, J.W. Suk, J.R. Potts, R.S. Ruoff, Graphene and graphene oxide: synthesis, properties, and applications, *Adv. Mater.*, 22 (2010) 3906–3924.
- [9] S. Park, R.S. Ruoff, Chemical methods for the production of graphenes, *Nat. Nanotechnol.*, 4 (2009) 217–224.
- [10] S. Stankovich, D.A. Dikin, R.D. Piner, K.A. Kohlhaas, A. Kleinhammes, Y. Jia, Y. Wu, S.T. Nguyen, R.S. Ruoff, Synthesis of graphene-based nanosheets via chemical reduction of exfoliated graphite oxide, *Carbon*, 45 (2007) 1558–1565.
- [11] D.V. Kosynkin, A.L. Higginbotham, A. Sinititskii, J.R. Lomeda, A. Dimiev, B.K. Price, J.M. Tour, Longitudinal unzipping of carbon nanotubes to form graphene nanoribbons, *Nature*, 458 (2009) 872–876.
- [12] A.H. Wazir, I.W. Kundi, Synthesis of graphene nano sheets by the rapid reduction of electrochemically exfoliated graphene oxide induced by microwaves, *J. Chem. Soc. Pak.*, 38 (2016) 11–16.
- [13] M.T. Tajabadi, W.J. Basirun, F. Lorestani, R. Zakaria, S. Baradaran, Y.M. Amin, M.R. Mahmoudian, M. Rezayi, M. Sookhikian, Nitrogen-doped graphene-silver nanodendrites for the non-enzymatic detection of hydrogen peroxide, *Electrochim. Acta*, 151 (2015) 126–133.
- [14] F. Chen, L. Guo, X. Zhang, Z.Y. Leong, S. Yang, H.Y. Yang, Nitrogen-doped graphene oxide for effectively removing boron ions from seawater, *Nanoscale*, 9 (2017) 326–333.
- [15] S. Zhou, N. Liu, Z. Wang, J. Zhao, Nitrogen-doped graphene on transition metal substrates as efficient bifunctional catalysts for oxygen reduction and oxygen evolution reactions, *ACS Appl. Mater. Interfaces*, 9 (2017) 22578–22587.
- [16] Q. Chen, X. Yang, Pyridinic nitrogen doped nanoporous graphene as desalination membrane: molecular simulation study, *J. Membr. Sci.*, 496 (2015) 108–117.
- [17] Y. Zhao, C. Zhang, T. Liu, R. Fan, Y. Sun, H. Tao, J. Xue, Low temperature green synthesis of sulfur-nitrogen co-doped graphene as efficient metal-free catalysts for oxygen reduction reaction, *Int. J. Electrochem. Sci.*, 12 (2017) 3537–3548.
- [18] P. Wu, Y. Qian, P. Du, H. Zhang, C. Cai, Facile synthesis of nitrogen-doped graphene for measuring the releasing process of hydrogen peroxide from living cells, *J. Mater. Chem.*, 22 (2012) 6402–6412.
- [19] M. Khan, M.N. Tahir, S.F. Adil, H.U. Khan, M.R.H. Siddiqui, A.A. Al-Warthan, W. Tremel, Graphene based metal and metal oxide nanocomposites: synthesis, properties and their applications, *J. Mater. Chem. A*, 3 (2015) 18753–18808.
- [20] C. Sun, B. Wen, B. Bai, Recent advances in nanoporous graphene membrane for gas separation and water purification, *Sci. Bull.*, 60 (2015) 1807–1823.
- [21] R. Zhang, X.-B. Cheng, C.-Z. Zhao, H.-J. Peng, J.-L. Shi, J.-Q. Huang, J. Wang, F. Wei, Q. Zhang, Conductive nano-structured scaffolds render low local current density to inhibit lithium dendrite growth, *Adv. Mater.*, 28 (2016) 2155–2166.
- [22] L. Liu, X. Guo, R. Tallon, X. Huang, J. Chen, Highly porous N-doped graphene nanosheets for rapid removal of heavy metals from water by capacitive deionization, *Chem. Commun.*, 53 (2017) 881–884.
- [23] X. Wang, P. Tang, C. Ding, X. Cao, S. Yuan, X. Zuo, X. Deng, Simultaneous enhancement of adsorption and peroxymonosulfate activation of Nitrogen-doped reduced graphene oxide for bisphenol A removal, *J. Environ. Chem. Eng.*, 5 (2017) 4291–4297.
- [24] P. Janik, B. Zawisza, E. Talik, R. Sitko, Selective adsorption and determination of hexavalent chromium ions using graphene oxide modified with amino silanes, *Microchim. Acta*, 185 (2018) 117–124.
- [25] I. Langmuir, The adsorption of gases on plane surfaces of glass, mica and platinum, *J. Am. Chem. Soc.*, 40 (1918) 1361–1403.
- [26] H.M.F. Freundlich, Über die adsorption in Lösungen [Over the adsorption in solution], *Z. Phys. Chem.*, 57 (1906) 385–470.
- [27] M.I. Temkin, V. Pyzhev, Kinetics of ammonia synthesis on promoted iron catalysts, *Acta Phys. Chim. USSR*, 12 (1940) 217–222.
- [28] M.M. Dubinin, L.V. Radushkevich, Equation of the characteristic curve of the activated charcoal, *Chem. Zentralbl.*, 1 (1947) 870–875.
- [29] S. Lagergren, About the theory of so-called adsorption of soluble substances, *K. Sven. Vetenskapsakad. Handl.*, 24 (1898) 1–39.
- [30] G. McKay, Y.S. Ho, Pseudo-second order model for sorption processes, *Process Biochem.*, 34 (1999) 451–465.
- [31] R.-S. Juang, M.-L. Chen, Application of the Elovich equation to the kinetics of metal sorption with solvent-impregnated resins, *Ind. Eng. Chem. Res.*, 36 (1997) 813–820.
- [32] W.J. Weber, J.C. Morris, Kinetics of adsorption on carbon from solution, *J. Sanitary Eng. Div.*, 89 (1963) 31–59.
- [33] T.C. Achee, W. Sun, J.T. Hope, S.G. Quitzau, C.B. Sweeney, S.A. Shah, T. Habib, M.J. Green, High-yield scalable graphene nanosheet production from compressed graphite using electrochemical exfoliation, *Sci. Rep.*, 8 (2018) 14525–14532.
- [34] P. Yu, S.E. Lowe, G.P. Simon, Y.L. Zhong, Electrochemical exfoliation of graphite and production of functional graphene, *Curr. Opin. Colloid Interface Sci.*, 20 (2015) 329–338.
- [35] Z. Aksu, E. Kabasakal, Batch adsorption of 2,4-dichlorophenoxyacetic acid (2,4-D) from aqueous solution by granular activated carbon, *Sep. Purif. Technol.*, 35 (2004) 223–240.
- [36] M. Forte, L. Mita, R. Perrone, S. Rossi, M. Argirò, D.G. Mita, M. Guida, M. Portaccio, T. Godievargova, Y. Ivanov, M.T. Tamer, A.M. Omer, M.S. Mohy Eldin, Removal of methylparaben from synthetic aqueous solutions using polyacrylonitrile beads: kinetic and equilibrium studies, *Environ. Sci. Pollut. Res.*, 24 (2017) 1270–1282.
- [37] S. Yu, X. Wang, W. Yao, J. Wang, Y. Ji, Y. Ai, A. Alsaedi, T. Hayat, X. Wang, Macroscopic, spectroscopic, and theoretical investigation for the interaction of phenol and naphthol on reduced graphene oxide, *Environ. Sci. Technol.*, 51 (2017) 3278–3286.
- [38] L. Dao, B. Xing, Adsorption of phenolic compounds by carbon nanotubes: role of aromaticity and substitution of hydroxyl groups, *Environ. Sci. Technol.*, 42 (2008) 7254–7259.
- [39] H.-W. Chen, C.-S. Chiou, S.-H. Chang, Comparison of methylparaben, ethylparaben and propylparaben adsorption onto magnetic nanoparticles with phenyl group, *Powder Technol.*, 311 (2017) 426–431.
- [40] H. Wang, Y. Chen, Y. Wei, A novel magnetic calcium silicate/graphene oxide composite material for selective adsorption of acridine orange from aqueous solutions, *RSC Adv.*, 6 (2016) 34770–34781.
- [41] B.H. Hameed, A.A. Rahman, Removal of phenol from aqueous solutions by adsorption onto activated carbon prepared from biomass material, *J. Hazard. Mater.*, 160 (2008) 576–581.
- [42] S. Yu, X. Wang, Y. Ai, X. Tan, T. Hayat, W. Hu, X. Wang, Experimental and theoretical studies on competitive adsorption of aromatic compounds on reduced graphene oxides, *J. Mater. Chem. A*, 4 (2016) 5654–5662.